Prediction of the elastic response of polymer based nanocomposites: a mean field approach and a discrete simulation

Emmanuelle Chabert, Rémy Dendievel, Catherine Gauthier, Jean-Yves Cavaillé

Prediction of the elastic response of polymer based nanocomposites: a mean field approach and a discrete simulation

E. Chabert[a,*], R. Dendievel[b], C. Gauthier[a], J.-Y. Cavaillé[a]

[a]*GEMPPM-INSA Lyon, 7 Avenue Capelle, 69621 Villeurbanne Cedex, France*
[b]*GPM2-INPG, 101 Rue de la Piscine, 38402 Saint Martin d'Heres Cedex, France*

The aim of this paper is to better understand mechanisms of reinforcement in particular nanocomposites, by studying the effects of filler ratio (varying from 0 to 45%) and strength of filler–filler interactions (either slightly or strongly bonded) on the viscoelastic behavior. Nanocomposites materials consisting, at room temperature, of submicronic rigid polysytrene (PS) particles randomly dispersed in a soft polybutylacrylate (PBA) polymeric matrix were obtained from mixtures of a film-forming PBA latex and a PS latex. Their viscoelastic behaviors have been characterized (i) after the film formation at room temperature and (ii) after an annealing treatment performed to enhance the interactions between neighboring PS particles (coalescence). The observed increase of elastic modulus and its evolution with temperature depend both on the filler ratio and on the strength of filler–filler interactions. Two micro-mechanical models have been then proposed to account for the short range interactions between filler particles: a self consistent scheme introducing a third rigidifying phase of matrix immobilized on the surface of filler particles, and a discrete model of sphere assembly taking into account the local contacts between filler/filler and matrix/filler. In addition to the good agreement with the experimental results, the discrete model highlighted the importance of filler–filler interactions on the reinforcement above the percolation threshold.

Keywords: A. Polymer-matrix composites; B. Mechanical properties; B. Modelling; C. Computational simulation; Percolation

1. Introduction

Polymer-based composites are constituted of two or more phases. Most of the time, they present one continuous phase (polymer matrix) in which another phase (filler) is dispersed at a microscopic scale. In this paper we are interested in polymer reinforced by submicronic particles (diameter $\approx$100 nm). The main characteristics of such materials, called nanocomposites, are (i) a very high interfacial area (about 10^8 m^2/m^3), and (ii) a very short distance between filler particles (about 10^{-8} m, which is approximately the giration radius of macromolecular chains). The last point suggests that almost all the matrix macromolecules are in contact with fillers. As a consequence, surface mechanisms (filler–filler and matrix–filler interactions), which are not clearly understood, are expected to play an important role in the mechanical behavior of nanocomposites.

In this paper, attention is focused on the effect of filler–filler interactions on the elastic properties of polymer-based nanocomposites. A convenient way to process nanocomposite materials is based on the mixture of various aqueous suspensions (colloids) [1–7]. Emulsion polymerization is well known to provide in a simple way polymer colloidal suspension with typical particle size in the range of ten to a few hundred nanometers. The morphology of such materials depend on the ability of the various polymer latexes to form a film [8]. When both colloids are film-forming, co-continuous systems are obtained. When only one suspension is film-forming (matrix), morphology type hard inclusion embedded in a soft matrix is achieved. Previous work of Favier [1] illustrates the importance of filler–filler interactions on the relaxed shear modulus of polymer filled

* Corresponding author at present address: LMS, Ecole Poly technique, 91128 Palaiseau Cedex. Tel.: +33-169-333318.
E-mail address: chabert@lms.polytechnique.fr (E. Chabert).

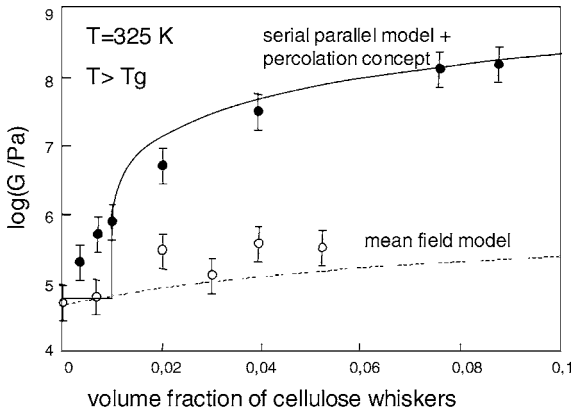

Fig. 1. Relaxed shear modulus of cellulose whiskers/poly(styrene-butyl acrylate) nanocomposites: (•) evaporation of blends of matrix and filler suspensions and (o) freeze-drying/ extrusion/hot pressing, from Ref. [1].

with cellulose whiskers. In that work, nanocomposites have been elaborated using two different routes (1) the latex route (film forming polymer and cellulose whiskers suspensions are blended and water evaporated), which leads to hydrogen bonding between whiskers; (2) freeze-drying/extrusion/hot pressing route, leading to almost no bonding between the whiskers. In Fig. 1, we observe that the shear modulus of "non interacting whiskers" composites (route 2) exhibits a smooth evolution, which can be accurately described by a mean field approach, whereas the shear modulus of the "interacting whiskers" composites (route 1) has been interpreted with the concept of percolation [9]. The very low percolation threshold is related to the large aspect ratio of the fillers (about 100).

When filler particles are spherical, the geometrical percolation occurs for higher filler content ($\phi \approx 20$ vol.%). The morphology of particular nanocomposites issued from mixtures of a film forming matrix latex and a non film forming filler latex might change as soon as temperature is increased and reaches the temperature of glass transition of the hard phase: clusters of hard particles or even long range filler network have been observed [10,11]. Several works have shown that this formation of a rigid network induced by a thermal treatment induces a significant increase of the elastic modulus [3,4,6,7].

Following these observations, we chose to study films issued from mixtures of polystyrene (PS, the filler) and polybutylacrylate (PBA, the matrix) latexes, which offer the possibility to vary easily the filler ratio (from 0 to 45 vol.%) and the strength of filler–filler interactions. In the first part, materials and dynamic mechanical experiments performed just after PBA maturation ("as dried" systems) and after an annealing treatment ("annealed" systems) are presented. In the second part, micro-mechanical modelling of elastic properties using (1) a generalised self consistent scheme and (2) a discrete numerical method are investigated and comparison of both methods is discussed.

2. Material and experimental results

Nanocomposites materials have been obtained from simple mixtures of a film-forming PBA latex ($T_g \approx -47$ °C) with a non film-forming PS latex ($T_g \approx 97$ °C), varying the amount of PS from 0 to 45%. These latexes have been elaborated through batch process, following the typical recipe: deionized water = 900 g, monomer = 90 g, $NaHC0_3$ = 0.75 g, initiator = 0.75 g ($K_2S_2O_8$ for PS and $(NH_4)_2S_2O_8$ for PBA), emulsifier = 2.91 phm of NC12 (3-(dimethyl dodecylammonium) propane-1-sulfonate) for PS, and 0.33 phm of sodium dodecyl sulfate for PBA. Temperature of polymerization = 70 °C.

Theses latexes have been mixed by hand in required proportions, and then the resulting mixtures were put in an oven during 2 weeks at 35 °C and 90% relative hygrometry. After water evaporation and film maturation, this process leads to rigid spherical PS fillers ($d = 110$ nm, as measured by dynamic light scattering) randomly dispersed in a soft PBA polymer matrix.

The dynamic shear moduli (G', G'') of the various nanocomposites have been measured as a function of temperature, with a homemade inverted pendulum working in a helium atmosphere. Experiments were performed in the temperature range (−170 to 150 °C) with a heating rate of 1 °C/min and at the fixed frequency of 1 Hz. In the following, G' and G'' are normalized by G'_0 the value measured at −100 °C.

Fig. 2 shows the isochronal viscoelastic behaviors of the pure matrix and the various PS-PBA composites obtained after the maturation process ("as dried" films). The dynamic mechanical response of a film of pure PS, elaborated by freeze-drying/hot pressing, is also reported. A significant reinforcement of shear modulus is observed in between PS and PBA main relaxations ($-42\ °C \leqslant T \leqslant 106\ °C$), i.e. when the contrast between PBA and PS moduli is more than three decades.

In addition to a higher level of relaxed modulus, the temperature evolution of composite moduli differs from that observed for the pure matrix and filler phase. The relaxed modulus of composite materials first decreases until approximately 70 °C, and then increases again until the PS main relaxation. The higher the filler content, the more pronounced these two counteracting phenomena. As consequences (i) these phenomena might be related to the interactions existing between matrix and filler and/or between filler particles, (ii) these interactions seem to evolve with temperature.

From the previous works mentioned above [3,4,6,7], the increase of modulus observed from ≈70 °C can be associated to the increase of interactions between

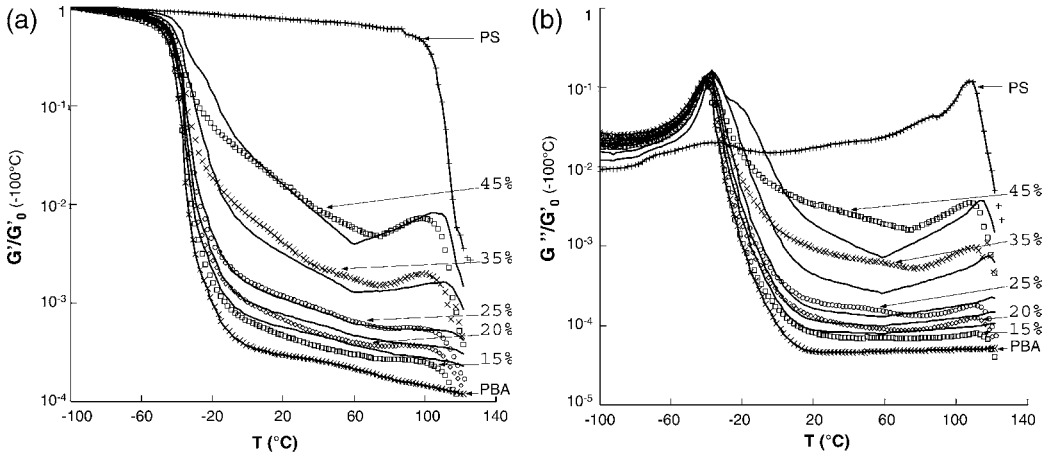

Fig. 2. Elastic shear modulus and loss shear modulus of "as dried" PS/PBA nanocomposites versus temperature for various PS contents. Dots: experiments (1 Hz, 1 °C/min). Lines: modelling using a generalised self consistent "four phase" model (Section 3), taking into account a vitreous matrix interphase between filler particles, whose thickness evolves with temperature ($e_{max} = 13.5$ nm [Eq. (1)], $T_1 = 0.85T_{\alpha(PS)}$ [Eq. (2)], $T_2 = 1.07T_{\alpha(PS)}$ [Eq. (2)]).

neighboring PS particles, may be due to an increase of the contact area by deformation of the spherical PS particles. This step should correspond to the very beginning of the coalescence (formation of a bonded neck by interdiffusion of macromolecular chains). To interpret the decrease of relaxed modulus in the low temperature range, we suggest that macromolecular chains anchored on the filler surface have less mobility than in the bulk matrix [12], and thus act as a rigidifying phase. The quantity of immobilized matrix decreases when temperature increases, leading to lower reinforcement.

Fig. 3 shows the dynamic modulus of the composites having undergone an annealing treatment at 140 °C during 4 h, to achieve the complete coalescence between neighboring PS particles, as it has been previously observed by TEM by Cavaille and co-workers [3,4]. The larger increase rate of the reinforcement is observed around ≈25% PS, i.e. near the geometrical percolation threshold. Compared with the viscoelastic behaviors of "as dried" films, annealed films exhibit a higher level of relaxed modulus, as it has been already pointed out by many works [3,4,6,7]. Moreover, the temperature dependance of relaxed moduli is similar to that of the pure PS. This indicates that the behavior of the nanocomposite is now governed by the stiff connected phase (PS).

These experimental results underline the difference in mechanical behavior between a system in which particles are just in contact ("as dried" systems), and a system in which particles are strongly bonded ("annealed" systems). In the following, two ways of micro-mechanical modeling are explored: homogenisation technique and discrete numerical method.

3. Modelling of "as dried" behaviors through homogenisation methods

In Section 2, we have made the assumption that the decrease of the relaxed modulus of PS–PBA systems is

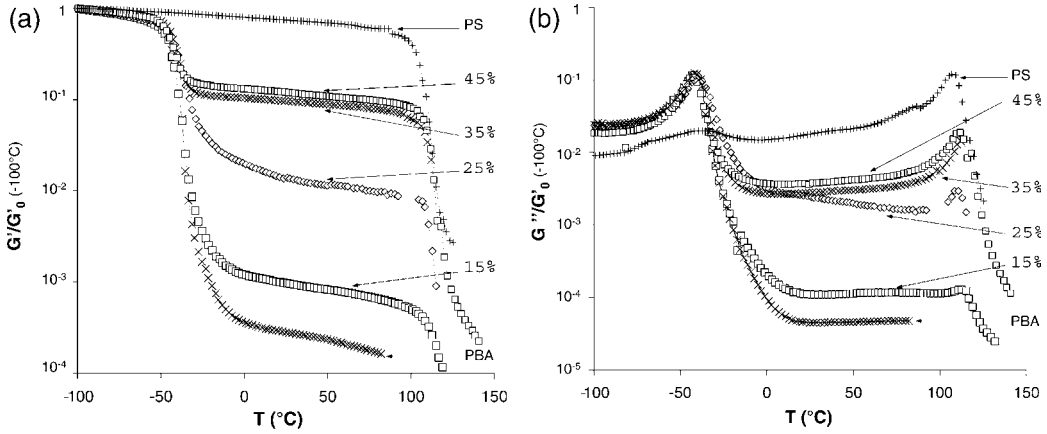

Fig. 3. Elastic shear modulus and loss shear modulus of "annealed" PS/PBA nanocomposites versus temperature for various PS contents (1 Hz, 1 °C/min).

related to the interphase existing between filler particle and the matrix. The properties of this interphase, if it exists, would change gradually from the filler surface to the bulk matrix, i.e. the temperature of main relaxation would change continuously.

This intermediate phase can be taken into account in a generalised self consistent scheme using a "four phase" representative volume element (RVE) [14] (Fig. 4), as done for instance in Ref. [13]. In this scheme, we consider that each PS particle is surrounded by a shell of vitreous matrix whose shear modulus is around 1 GPa; the thickness e of this shell decreases with temperature as macromolecular chains of the external layer reach their main relaxation. The thickness is then maximal ($e_{\max}$) below the temperature of main relaxation of pure PBA ($T_{\alpha(\mathrm{PBA})}$) and becomes zero at the temperature of main relaxation of pure PS ($T_{\alpha(\mathrm{PS})}$). For sake of simplicity, we chose a linear decrease between the two temperatures:

$$e(T) = e_{\max}\frac{T_{\alpha(\mathrm{PS})} - T}{T_{\alpha(\mathrm{PS})} - T_{\alpha(\mathrm{PBA})}} \quad (1)$$

In addition, the beginning of coalescence between neighboring particles induces an increase of modulus from 70 °C approximately. The representative morphological motif used here (concentric layers) does not enable to take into account the growing connectivity between PS particles. However, to account for these effects, it is possible to increase artificially the filler ratio. From the experiments plotted in Fig. 2, one can suppose that the coalescence of PS particles starts at $T_1 \approx 0.8 T_{\alpha(\mathrm{PS})}$ and grows in the temperature range concerned in this study (until $T_2 \approx 1.2 T_{\alpha(\mathrm{PS})}$ approximately). Above T_2, the increase of composite rigidity is masked by the softening of PS particles during their main relaxation. The increase of the thickness e from T_1 until T_2 is also chosen linear:

$$e(T)_{(T>T_1)} = e(T_1) - [e(T_1) - e_{\max}]\frac{T - T_1}{T_2 - T_1} \quad (2)$$

To avoid possible misunderstanding, we reiterate that the interphase has distinct origins at low and at high temperature: it represents either the immobilized matrix (low temperature) or an artificially extra phase of PS (high temperature). In both cases, the modulus is taken equal to 1 GPa.

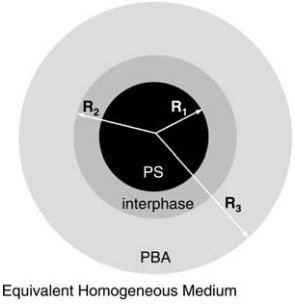

Fig. 4. Four phase representative volume element (RVE) used in the mean field approach.

In this modelling, the only adjustable parameter is the thickness $e_{\max}$ of vitreous interphase surrounding PS particles (whatever the PS concentration is) at the main relaxation temperature of pure PBA. Calculations of shear moduli $G'(T)$ and $G''(T)$ have been made according to Ref. [14]. The different radii R_1, R_2 and R_3 of the four phase representative morphological motif (Fig. 4) are linked to the PS concentration (ϕ), the PS particle radius ($r_{PS} = 55$ nm) and the thickness of interphase $e(T)$ through: $R_1 = \phi^{\frac{1}{3}}$, $R_2 = \phi^{\frac{1}{3}}\,(1 + e(T)/r_{PS})$ and $R_3 = 1$. Equations have been solved considering that the compressibility modulus K of polymers remains about constant with temperature (taking a Poisson ratio equal to 0.32 in the vitreous state [15] and $G' = 1$ GPa at -100 °C gives $K = 2.4$ GPa). The best agreement is obtained for $e_{\max} = 13.5$ nm. Within this assumption, the whole viscoelastic behavior [$G'(T)$, $G''(T)$] of all "as dried" materials is correctly described, as shown in Fig. 2.

Although the effective concentration of filler becomes very large (see Table 1), the value of $e_{\max}$ is reasonable from a physical point of view: taking a typical value for the polymerization degree of polymer synthesised by emulsion $10^2 < D_p < 10^4$ and a length of PBA repetition unit of the order of 5 Å, leads to an average quadratic giration radius of macromolecular chains ranging between 2 and 20 nm.

The interphase thickness $e_{\max}$ has been here determined by inverse method, in order to get a good agreement with all experimental data. A great sensibility of this parameter on the calculated curves has been observed. If this interphase is not taken into account, estimated moduli are really too weak compared with experimental ones. As a conclusion, this interphase seems to playa major role in the mechanical behavior of nanocomposites.

4. Discrete numerical simulation

Experimental results have shown a large evolution of mechanical properties induced by a thermal treatment.

Table 1
Comparison between PS concentration and effective filler concentration at $T_{\alpha(\mathrm{PBA})}$ taking into account a vitreous interphase in homogenization methods

Concentration of PS	0	0.15	0.20	0.25	0.35	0.45	1
Effective filler concentration at $T_{\alpha(\mathrm{PBA})}$	0	0.27	0.37	0.46	0.64	0.83[a]	1

[a] Value above the random close packing compacity.

To model these effects, it is necessary to take into account the nature of contacts (small area geometrical contact before the annealing treatment or strongly bonded contact after the annealing treatment) and the microstructure. In this aim, a discrete numerical simulation has been developed, based on composite particle assembly calculations with linear relations representing the contact behavior. We used in fact a scheme developed by Jagota [16,17] to model the viscosity of composite packings of soft and hard spheres. The algorithm of simulation is divided into two parts: (1) generation of a packing of spheres and geometrical treatment, and (2) numerical resolution of equilibrium equations.

4.1. Particle assembly

A compact assembly of approximately 10 000 mono disperse rigid spheres is generated using a gravity deposition type algorithm described in Ref. [18]. The packing compacity c is around 0.57, and the average coordination number is 6. In order to avoid edges effects, calculations are carried out on a subset of $N \approx 1000$ spheres among which are randomly chosen hard (PS fillers) and soft (PBA matrix) spheres [Fig. 5(a)].

4.2. Mechanical interactions and packing modulus

Equations given for the viscosity in Ref. [17] are here transposed for the elastic modulus. Force transmission at each contact between two particles i and j is defined, in a local orthonormal reference ($\boldsymbol{n}$, $\boldsymbol{t_1}$, $\boldsymbol{t_2}$), by a system of six linear equations connecting the three forces $\boldsymbol{F^{ij}}$ and the three moments $\boldsymbol{M^{ij}}$ transmitted through the contact to the displacements ($\mathbf{\Delta u_i}$, $\mathbf{\Delta u_j}$) and the rotations ($\mathbf{\Delta \theta_i}$, $\mathbf{\Delta \theta_j}$) of spheres [Fig. 5(b)]:

$$\begin{cases} F_{\mathrm{n}}^{ij} = k_{\mathrm{n}}\left(\dfrac{\Delta u_{\mathrm{n}}^{j} - \Delta u_{\mathrm{n}}^{i}}{2R}\right) \\ F_{\mathrm{t1}}^{ij} = k_{\mathrm{t}}\left(\dfrac{\Delta u_{\mathrm{t1}}^{j} - \Delta u_{\mathrm{t1}}^{i}}{2R}\right) - \dfrac{k_{\mathrm{t}}}{2}\left(\Delta\theta_{\mathrm{t2}}^{j} + \Delta\theta_{\mathrm{t2}}^{i}\right) \\ F_{t2}^{ij} = k_{\mathrm{t}}\left(\dfrac{\Delta u_{\mathrm{t2}}^{j} - \Delta u_{t2}^{i}}{2R}\right) + \dfrac{k_{\mathrm{t}}}{2}\left(\Delta\theta_{\mathrm{t1}}^{j} + \Delta\theta_{\mathrm{t1}}^{i}\right) \\ \dfrac{M_{\mathrm{n}}^{ij}}{R} = \dfrac{k_{\theta}}{2}\left(\Delta\theta_{\mathrm{n}}^{j} - \Delta\theta_{\mathrm{n}}^{i}\right) \\ \dfrac{M_{\mathrm{t_1}}^{ij}}{R} = -F_{\mathrm{t_2}}^{ij} + \dfrac{k_{\mathrm{b}}}{2}\left(\Delta\theta_{\mathrm{t_1}}^{j} - \Delta\theta_{\mathrm{t_1}}^{i}\right) \\ \dfrac{M_{\mathrm{t_2}}^{ij}}{R} = -F_{\mathrm{t_1}}^{ij} + \dfrac{k_{\mathrm{b}}}{2}\left(\Delta\theta_{\mathrm{t_2}}^{j} - \Delta\theta_{\mathrm{t_2}}^{i}\right) \end{cases} \tag{3}$$

These linear contacts laws are characterized by k_n, k_t, k_e and k_b, respectively normal, tangential, bending and torsion "stiffness" (these contact stiffnesses have in fact the dimension of a force).

The various contact stiffnesses depend only on material properties (elastic modulus G) and on the geometry of contact through [17]:

$$\begin{cases} k_{\mathrm{n}} = 3G\pi R^2\sqrt{\alpha} \\ k_{\mathrm{t}} = k_{\mathrm{n}}/3 \\ k_{\mathrm{b}} = \dfrac{9}{4}k_t\alpha \\ k_{\theta} = k_{\mathrm{b}}/3 \end{cases} \tag{4}$$

where R_c is the contact radius, R is the sphere radius and α denotes the ratio $\alpha = (R_c/R)^2$.

The equations of contact [Eq. (3)], added to the force and moment equilibrium equations of each particles, lead to a system of $6N$ linear equations whose unknown are the displacements and the rotations of each sphere. Boundary conditions corresponding to a classical com-

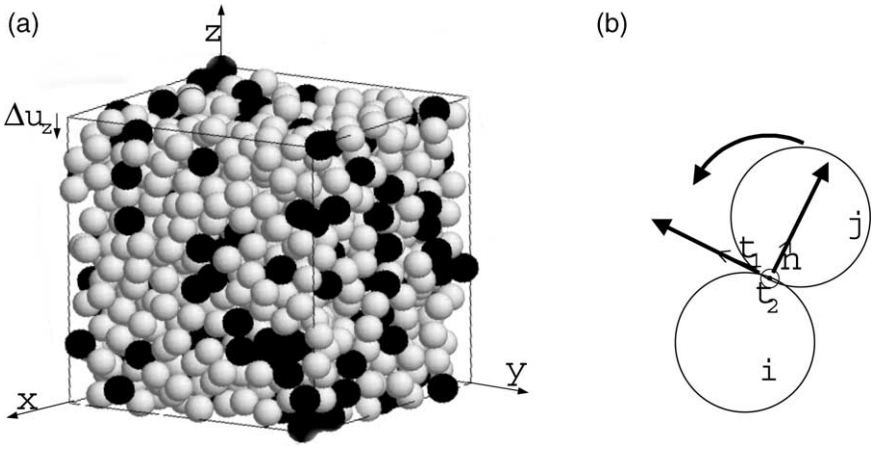

Fig. 5. (a) Random packing of equal-sized hard and soft spheres. Such packings are used to calculate the effective moduli by subjecting them to appropriate boundary conditions. (b) Transmission of normal and tangential efforts and moments between two spheres i and j.

pression test are applied: spheres of the upper face of the packing are submitted to a vertical displacement, while spheres of the lower face are fixed in their horizontal plane (except one which is totally fixed to avoid a rigid body displacement). The longitudinal modulus M_l is numerically determined by the ratio of the resulting force with the applied displacement. In order to recover the modulus of the bulk matrix G_m when the packing contains only soft spheres, M_l is normalized by the ratio M_l^0/G_m; M_l^0 being the packing modulus of a soft particles assembly. The normalised modulus of the packing G is thus given by:

$$G = \frac{M_l}{M_l^0} G_m \tag{5}$$

4.3. Interactions in composite packing

The major interest of this numerical simulation is to take explicitly into account the short range interactions between filler particles and between matrix and filler. Three kinds of contacts are thus considered: soft/soft (ss), hard/hard (hh) and hard/soft (hs):

1. Soft/soft contacts are characterized by the matrix modulus G_{PBA} and by the radius of soft/soft contact R_c^{ss} (Eq. 4). As the matrix of nanocomposites is continuous, the contact radius of soft spheres is here approximated by the radius of the spheres themselves: $R_c^{ss} = R$.
2. Hard/hard contacts are characterized by a modulus G_{PS} and a contact radius R_c^{hh} (Eq. 4). The key parameter in these contact equations is α ($\alpha = \left(R_c^{hh}/R\right)^2$), which in fact represents, above its geometrical aspect, the ability to transmit moments trough the contact. When $\alpha = 1$, the contact transmits bending and torsion moments as well as normal and tangential forces. When α decreases, bending and torsional efforts are less transmitted than normal and tangential efforts. We will let vary α, i.e. the contact radius between hard spheres R_c^{hh}, on a broad range in order to quantify the effect of filler-filler interactions on the modulus packing.
3. Hard/soft contacts result from a serial law between hard/hard contacts and hard/soft contacts. Assuming that the matrix totally wets filler particles, we fixe the contact radii between soft and hard particles to the radius of the spheres themselves: $R_c^{hs} = R$. In case of high contrast between matrix and filler moduli, this gives: $k_n^{hs} = 2k_n^{ss}$.

4.4. Comparison with experimental results

In order to compare the discrete simulation with the experimental results, a preliminary problem has to be overcome. In the first case, the results are obtained as a function of the site fraction of hard spheres in the mixture. One has to give a correspondance between this site fraction p and the volume fraction ϕ of PS particles. The relation linking these two fractions is not trivial. Since the matrix is continuous and the fillers are spherical, the volume of voids in the packing can be considered, in a first approximation, as being filled by the matrix phase:

$$\phi = cp \tag{6}$$

where $c = 0.57$ is the packing compacity. This assumption leads to a classical value of the geometrical percolation threshold (0.325 in sites gives 0.185 in volume) [19]. However, the modulus of pure PS material G_{PS} is obtained for 57 vol.% of hard spheres (when $\alpha = 1$). Eq. (6) tends then to overestimate elastic properties from $\phi \approx 40\%$ [value at which the packing modulus exceeds Hashin and Shtrikman upper bound, as shown in Fig. 6(b)]. To avoid that, a possible correction would to gradually fill interstices by the filler phase, for example those who are surrounded only by hard particles (each interstice being surrounded by six spheres, the probability of having a filler interstice is then p^6). This correction, valid for $\alpha = 1$, gives [20]:

$$\phi = 0.57p + 0.43p^6 \tag{7}$$

with this relation plotted in Fig. 6(a), the effective modulus can be thus obtained for ϕ ranging from 0 to 1 when $\alpha = 1$ [Fig. 6(b)].

4.5. "Annealed" films

After the annealing treatment, neighboring PS particles are strongly bonded. As a consequence, the elastic properties of "annealed" films are modeled by considering an interaction maximum between hard particles, i.e. $\alpha = 1$ (efforts and moments are transmitted as in bulk PS). As shown in Fig. 7, simulations are in quite good agreement with experimental data for 15, 25, 35 and 45% PS. It is worth noticing that the agreement is obtained without any adjustable parameter.

4.6. "As dried" films

Before the annealing treatment, the strength of filler–filler interactions evolves with temperature, according to the two physical assumptions discussed in Section 2:

1. In the low temperature range ($T_{\alpha(PBA)} \leqslant T \leqslant$ 70 °C), the matrix present in the confined zones drawn on Fig. 8, is assumed to be vitreous. The equilibrium between confined and non confined zones is temperature dependent. We chose an arrhenian law to describe the decrease of the quantity of vitreous matrix, which is directly related to α, when the temperature increases.

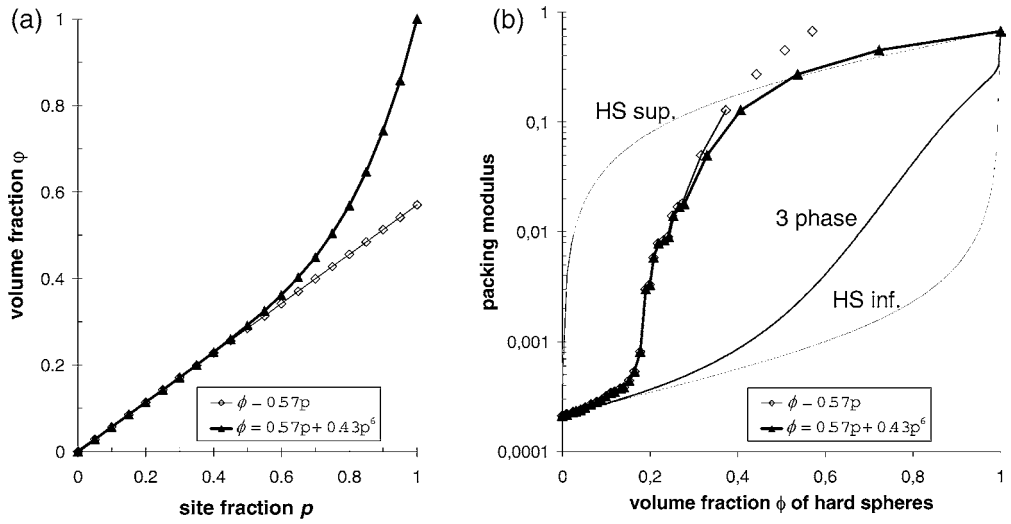

Fig. 6. (a) Relation between the site fraction p and the volume fraction ϕ (◇) Eq. (6) and (▲) Eq. (7) (for $\alpha = 1$). (b) Evolution of assembly modulus as a function of volume fraction ϕ of filler (1000 spheres, contrast $G_{PS}/G_{PBA} = 3150$ obtained at 60 °C in PS–PBA nanocomposites, $\alpha = 1$). Comparison with Hashin and Shtrikman bounds and the "three phase" self consistent model [14]. Eq. (6) is no more valid for $\phi > 0.4$ when $\alpha \approx 1$.

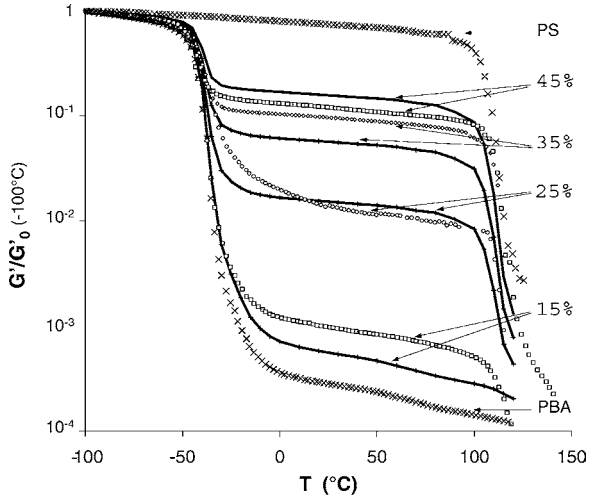

Fig. 7. Simulation (—) of the real shear modulus of "annealed" PS–PBA nanocomposites compared to experimental data (dots). Calculations are made on a packing of 1000 spheres, considering a maximal interaction between PS particles ($\alpha = 1$).

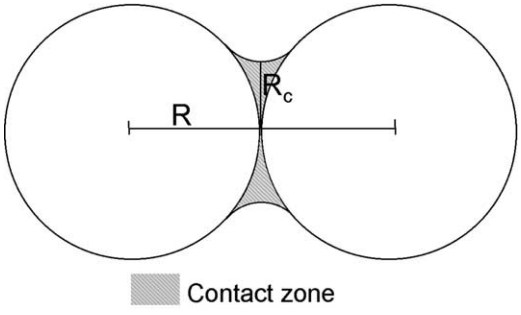

Fig. 8. Contact area between PS particles. R_c is the contact radius.

2. In the high temperature range (70 °C $\leqslant T \leqslant$ $T_{\alpha(PS)}$), the coalescence between neighboring PS particles begins to occur, leading to higher contact radius. This process being thermally activated, an arrhenian law is also chosen to describe the increase of $\alpha(T)$.

The parameters of the two arrhenian laws have been adjusted in order to get a good agreement for the temperature evolution of the real shear modulus of the composite containing 25% PS:

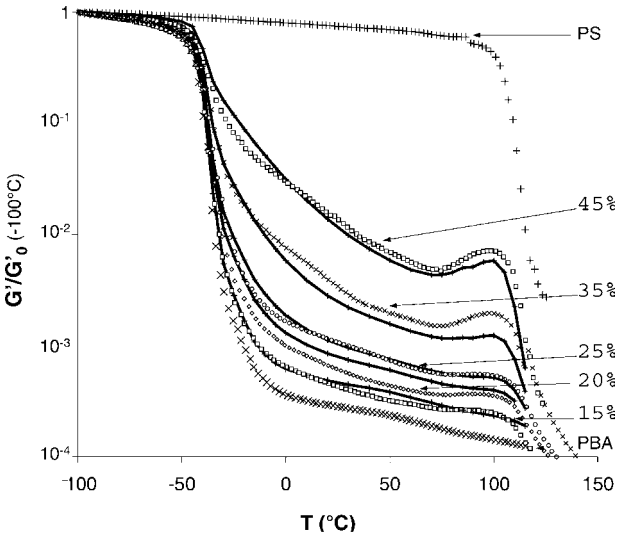

Fig. 9. Simulation (—) of the real shear modulus of "as dried" PS–PBA nanocomposites compared to experimental data (dots). Calculations are made on a packing of 1000 spheres, considering a "bonded" contact and a ratio $\alpha(T) = (R_c^{hh}(T)/R)^2$ evolving with temperature [Eq. (8)].

$$\alpha(T) = 4.7 \times 10^{-10}\exp\left(\frac{40390}{RT}\right) + 3 \times 10^{9}\exp\left(\frac{-83394}{RT}\right) \quad (8)$$

with this law, α decreases from approximately 10^{-1} to 10^{-3} above the temperature of main relaxation of PBA, and increases again from 10^{-3} to 2.10^{-2} above $T \approx 65$ °C.

The effective moduli of the other nanocomposites materials have been simulated with the evolution of $\alpha(T)$ given by Eq. (8). As shown on Fig. 9, simulation results are in very good agreement with experimental data, for all PS compositions.

5. Conclusion

The experimental results and the micro-mechanical modellings presented in this paper have shown that filler–filler interactions have a large influence on the elastic properties of nanocomposites, either via vitreous matrix at the interface (''as dried'' systems), or via bonds between filler particles (''annealed'' systems).

Two kinds of modeling have been proposed to describe the isochronal elastic behaviors of ''as dried'' nanocomposites. The physical bases are the same in the two modellings, but they are treated differently: in homogenisation scheme, the thickness of interphase (or effective volume of filler) is the key parameter, whereas in the discrete simulation, the surface of contact (or interaction forces) between filler particles rules the mechanical behavior. Thus, it is necessary to increase considerably the effective fraction of filler in the self-consistent model to account for the observed reinforcement, whereas in discrete simulation, a slight volume of immobilized matrix confined between filler particles, leads to a significant increase of the modulus. It arises that it is now essential to obtain more information on this vitreous matrix, for instance by performing molecular dynamics calculations and/or solid state NMR experiments.

Anyway, the self-consistent scheme proposed here is not valid for ''annealed'' materials since the macroscopic filler network is not taken into account. In that case, considering a maximal interaction between PS particles after coalescence, the discrete numerical simulation succeeds very well in describing the modulus increase. Moreover, this simulation clarifies the concept of mechanical percolation: contrary to geometrical percolation, mechanical percolation only occurs when moments are transmitted.

Acknowledgements

This work was performed under the auspices of ''Programme Materiaux'' from CNRS under contract no. 113. One of the authors (E. Chabert) was supported through the Brite project BE 97-4448 administrated by the European Community. C. Graillat is also gratefully acknowledged for providing technical help and fruitful discussion.

References

[1] Favier V, Dendievel R, Canova G, Cavaille J-Y, Gilormini P. Simulation and modeling of three dimensional percolating structures: case of a latex matrix reinforced by a network of cellulose fibers. Acta Mater 1997;45:1557–65.

[2] Eckersley ST, Helmer BJ. Mechanistic considerations of particle size effects on film properties of hard/soft latex blends. J Coat Technol 1997;69:97–107.

[3] Cavaille J-Y, Vassoille R, Thollet G. Structural morphology of poly(styrene)-poly(butyl acrylate) polymer-polymer composites studied by dynamic mechanical measurements. Colloid Polym Sci 1991;269:148–258.

[4] Hidalgo M, Cavaille J-Y, Guillot J. Polystyrene (1)/ poly(butyl acrylatemethacrylic acid) (2) core-shell emulsion polymers. Part II: thermomechanical properties of latex films. Colloid Polym Sci 1992;270:1208–21.

[5] Agarwal N, Farris RJ. Thermodynamics of deformation of latex blend coatings and its implications for tailoring their properties. J Coat Technol 1999;71:61–72.

[6] Oconnor KM, Tsaur SL. Phase rearrangement in two-stage emulsion polymers of butyl acrylate and styrene: mechanical properties. J Appl Polym Sci 1987;33:2007–27.

[7] Richard J. Thermomechanical behaviour of composite polymer films obtained from poly(vinyl acetate) latexes sterically stabilized by poly(vinyl alcohol). Polymer 1993;34:3823–31.

[8] Steward PA, Hearn J, Wilkinsopn MC. An overview of polymer latex film formation and properties. Adv Colloid Interface Sci 2000;86:195–267.

[9] Ouali N, Cavaille J-Y, Perez J. Elastic, viscoelastic and plastic behavior of multiphase polymer blends. Plast Rubber Compos Process Appl 1991;16:5560.

[10] Feng J, Winnick MA, Shivers R. Polymer blend latex films: morphology and transparency. Macromolecules 1995;32:7671–82.

[11] Chevalier Y, Hidalgo M, Cavaille J-Y. Structure of waterborne organic composite coatings. Macromolecules 1999;32:7887–96.

[12] De Gennes PG. La matiere ultradivisee. In: L'ordre du chaos Berlin: Bibliotheque pour la science. 1989, p. 128–35.

[13] Colombini D, Maurer FHJ. Origin of the additional mechanical transitions in multicomponent polymeric materials. Macromolecules 2002;35:5891–902.

[14] Herve E, Zaoui A. Elastic behaviour of multiply coated fibre-reinforced composites. Int J Eng Sci 1993;31:1–10.

[15] Nielsen LE, Landel RF. Mechanical properties of polymers and composites. 2nd ed. New York: M Dekker; 1994.

[16] Jagota A, Sherer GW. Viscosities and sintering rates of two-dimensional granular composites. J Am Chem Soc 1993;76:3123–35.

[17] Jagota A, Sherer GW. Viscosities and sintering rates of composites packings of spheres. J Am Chem Soc 1995;78:521–8.

[18] Bouvard D, Lange FF. Relation between percolation and particle coordination in binary powder mixtures. Acta Metall Mater 1991;39:3083–90.

[19] Stauffer D. Introduction to percolation theory. London: Taylor and Francis; 1985.

[20] Chabert E. Nanocomposites à matrice polymère: approche expérimentale et modélisation. PhD thesis, INSA Lyon, 2002.